OG 2.1.14

On the conversion of blast wave energy into radiation in AGNs and GRBs

M. Pohl, R. Schlickeiser
Institut für Theoretische Physik IV, Ruhr-Universität Bochum, 44780 Bochum, Germany

Abstract

It has been suggested that relativistic blast waves may power the jets of AGN and Gamma-ray bursts. We address the important issue how the kinetic energy of collimated blast waves is converted into radiation. It is shown that swept-up ambient matter is quickly isotropised in the blast wave frame by a relativistic two-stream instability, which provides relativistic particles in the jet without invoking any acceleration process. The fate of the blast wave and the spectral evolution of the emission of the energetic particles is therefore solely determined by the initial condition. We compare our model with existing multiwavelength data of AGN and find remarkable agreement.

1 Introduction

Published models for the γ-ray emission of blazars are usually based on interactions of highly relativistic electrons of unspecified origin. The usual shock or stochastic electron acceleration processes would have to be very fast to compete efficiently with the radiative losses at high electron energies, and a high energy cut-off should occur under realistic conditions, but no low energy cut-off, in contrast to the results of the spectral modeling. Energetic electrons may also result from photomeson production of highly relativistic protons, but the observed short variability timescale places extreme constraints on the magnetic field strength, for the proton gyroradius has to be much smaller than the system itself, and on the Doppler factor, for the intrinsic timescale for switching off the cascade is linked to the observed soft photon flux.

In this paper we consider a strong electron-proton beam that sweeps up ambient matter and thus becomes enriched with relativistic particles. We shall address the important issue how the kinetic energy of such channelled relativistic blast waves is converted into radiation. Existing fireball models of GRBs and AGNs (see e.g. Vietri 1997; Waxman 1997; Böttcher and Dermer 1998) are very unspecific on this crucial point. Viewed from the coordinate system comoving with the blast wave, the interstellar protons and electrons represent a proton-electron beam propagating with relativistic speed antiparallel to the x-axis. We demonstrate that very quickly the beam excites low-frequency magnetohydrodynamic plasma waves via a two-stream instability which isotropise the incoming interstellar protons and electrons in the blast wave plasma. Inelastic collisions between primary protons and the blast wave protons generate neutral and charged pions which decay into gamma rays, secondary electrons, positrons and neutrinos. Both, the radiation products from these interactions, and the resulting cooling of the primary particles in the blast wave plasma, are calculated. By transforming to the laboratory frame we calculate the time evolution of the emitted multiwavelength spectrum for an outside observer under different viewing angles. The deceleration of the blast wave is taken into account self-consistently. Since we do not consider any re-acceleration of particles in the blast wave, the evolution of particles and the blast wave is completely determined by the initial conditions.

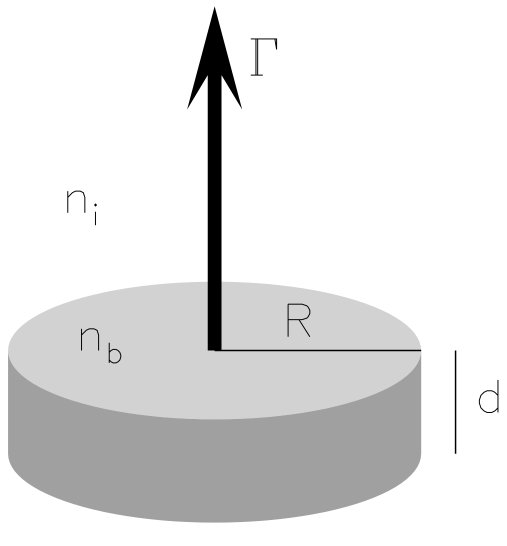

Figure 1: Sketch of the basic geometry. The thickness of the channeled blast wave d is much smaller than its halfdiameter R. The blast wave moves with a bulk Lorentz factor Γ through ambient matter of density n_i.

2 Two-stream instability of a proton-electron beam

As sketched in Fig. 1 we consider in the laboratory frame (all physical quantities in this system are indexed with $*$) the cold blast wave electron-proton plasma of density n_b^* and thickness d^* in x-direction running into the cold interstellar medium of density n_0^*, consisting also of electrons and protons, parallel to the uniform magnetic field of strength B. In the comoving frame the total phase space distribution function of the plasma in the blast wave region at the start thus is

$$f(p,t=0) = \frac{1}{2\pi p^2} n_i \delta(\mu+1)\delta(p-P) + \frac{1}{4\pi p^2} n_b \delta(p) = n_b f_b(p,\mu,t=0) + n_i f_i(p,\mu,t) \;, \quad (1)$$

where $P = \Gamma m V = \Gamma m \beta c = mc\sqrt{\Gamma^2-1)}$, $\mu = p_{\|}/p$. If the beam distribution function f_i in Eq. (1) is unstable it excites plasma waves. The time-dependent behaviour of the intensities $I(k,t)$ of the excited waves is given by $\frac{\partial I_\pm}{\partial t} = \pm\psi I_\pm$ where the growth rate ψ is

$$\psi(k) \simeq \pi^2 c^3 [\frac{\partial J(\omega_R)}{\partial \omega_R}]^{-1} \mathrm{sgn(k)} \sum_{\mathrm{i}} \omega_{\mathrm{p,i}}^2 (\mathrm{m_i c})^3 \int_{\mathrm{E_i}}^{\infty} \mathrm{dE}\, \frac{\mathrm{E^2 - 1 - (\frac{E}{N} - x_i)^2}}{\sqrt{\mathrm{E^2-1}}} \frac{\partial \mathrm{f_i}}{\partial \mu} \delta(\mu + \frac{\mathrm{x_i}}{\sqrt{\mathrm{E^2-1}}}) \;, \quad (2)$$

and $N = ck/\omega_R$ is the index of refraction, and $E_i = \sqrt{1+x_i^2}$ with $x_i = \Omega_{i,0}/kc$. To describe the influence of these excited waves on the beam particles we use the quasilinear Fokker-Planck equation (e.g. Schlickeiser 1989) for the resonant wave-particle interaction. We concentrate here on Alfven waves mainly for two reasons:
(1) the bulk of the momentum of the inflowing interstellar particles is carried by the protons so that they are energetically more important than the electrons;
(2) for Lorentz factors $\Gamma > |\mu| m_p/m_e$ the isotropisation of electrons is also due to scattering with Alfven waves; for smaller Lorentzfactors the mistake one makes in representing the Whistler dispersion relation still by the Alfven dispersion relation is relatively small.

For Alfven waves the index of refraction is large compared to unity, so that the Lorentz force associated with the magnetic field of the waves is much larger than the Lorentz force associated with the electric field, so that on the shortest time scale these waves scatter the particles in pitch angle μ but conserve their energy, i.e. the isotropise the beam particles. The Fokker-Planck equation for the phase space density then displays only a term for pitch angle scattering with

$$D_{\mu\mu} \simeq \sum_n \frac{\pi\, \Omega_i^2\, (1-\mu^2)}{2\, B^2} \int_{-\infty}^{\infty} dk\, I_n(k) \delta(\omega_R - kv\mu - \Omega_i) \quad (3)$$

Now it is convenient to introduce the normalised phase space distribution function of the beam particles

$$f_i(p,\mu,t) = \frac{\delta(E-\Gamma)}{2\pi(m_i c)^3 \Gamma(\Gamma^2-1)^{1/2}} F_i(\mu,t) \;, \quad (4)$$

where $E = \sqrt{1+(p/mc)^2}$. Summing over protons and electrons separately, and introducing the proton and electron Larmor radii, $R_p = c\sqrt{\Gamma^2-1}/\Omega_p$, $R_e = c\sqrt{\Gamma^2-1}/|\Omega_e|$, respectively, we finally obtain

$$I_+(t)I_-(t) = I_+(t=0)I_-(t=0) \quad \text{and} \quad [I_+(t)-I_-(t)] - [I_+(t=0)-I_-(t=0)] = Z(k) \quad (5)$$

with

$$Z(k) = \frac{m_e}{m_p} \frac{b(|k|)}{a_p(|R_p k|^{-1})} [1-(kR_p)^{-2}] \sum_{x=e,p} H[|k|-R_x^{-1}] \int_{-1}^{-\mathrm{sgn}(\Omega_{x,0})/R_x k} d\mu [F_x(\mu,t) - F_x(\mu,t=0)] \quad (6)$$

The distribution functions of the beam particle i evolve according to

$$\frac{\partial F_i}{\partial t} = \frac{\partial}{\partial \mu}[a_i(|\mu|) \sum_{\pm} I_\pm(|R_i \mu|^{-1}) \frac{\partial F_i}{\partial \mu}] \quad \text{with} \quad a_i(|\mu|) \equiv \frac{\pi}{2} \frac{v(1-\mu^2)}{B^2 R_i^2 |\mu|} \quad (7)$$

We can estimate the isotropisation length by using the fully-developed turbulence spectra for calculating the pitch angle Fokker-Planck coefficient. For ease of exposition we assume that the initial turbulence spectrum has the form $I(k,0) = I_0 k^{-2}$. As a consequence of pitch-angle scattering the beam particles adjusts to the isotropic distribution on a length scale given by the scattering length $\lambda = \frac{3v}{8}\int_{-1}^{1} d\mu \frac{(1-\mu^2)^2}{D_{\mu\mu}(\mu)}$. After staightforward but tedious integration and inserting our typical parameter values we obtain for the scattering length and the isotropisation time scale in the blast wave plasma

$$\lambda \simeq 10^{11}\, \frac{n_{b,8}^{1/2}}{\Gamma_{100}\, n_i^*} \quad \mathrm{cm} \quad \text{and} \quad \mathrm{t_R} = \lambda/\mathrm{c} = 3.5\, \frac{\mathrm{n_{b,8}^{1/2}}}{\Gamma_{100}\, \mathrm{n_i^*}} \quad \mathrm{s} \tag{8}$$

If the thickness d of the blast wave region is larger than the scattering length, indeed an isotropic distribution of the inflowing interstellar protons and electrons with Lorentzfactor $< \Gamma >= \Gamma(1-\beta_A \beta) \simeq \Gamma$ in the blast wave frame is efficiently generated. In the following sections we investigate the radiation products resulting from the inelastic interactions of these primary particles with the cold blast wave plasma.

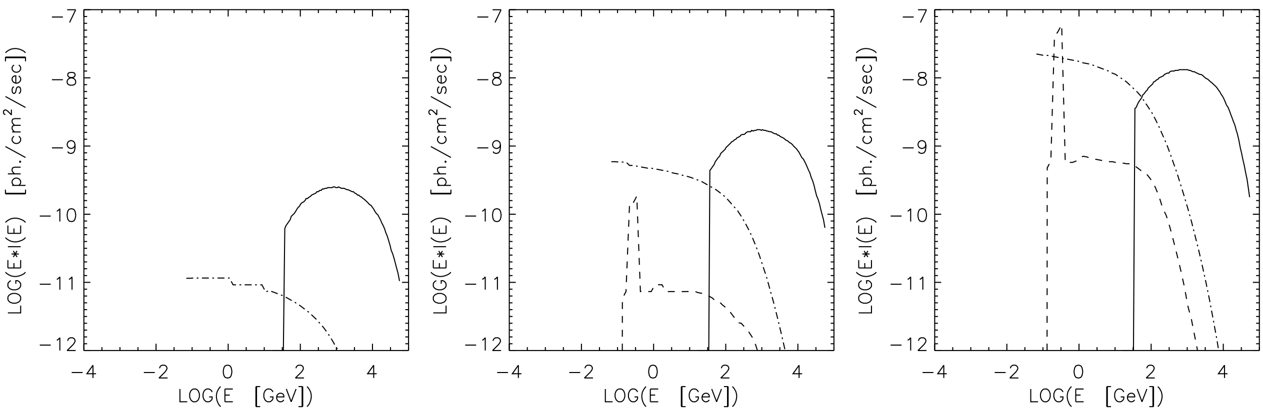

Figure 2: Spectral evolution of a relativistic blast wave in an environment of constant density. The solid line displays π^0-decay γ-rays , the dot-dashed line bremsstrahlung, and the dashed line annihilation emission. From left to right the panels show the spectra after 50 seconds, 500 seconds, and 5000 seconds observed time. The parameters are: Γ_0=300, d=$5 \cdot 10^{12}$cm, R=10^{15}cm, B= 1 G, n_i=0.01 cm^{-3}, n_b=$4 \cdot 10^8$ cm^{-3}, for an AGN at z=0.1 viewed at an angle μ=1.

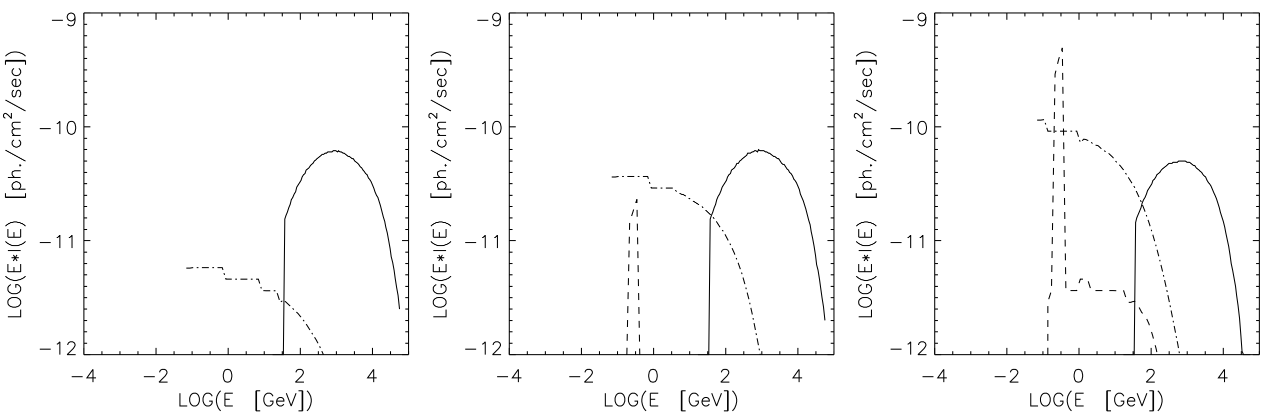

Figure 3: Spectral evolution of a relativistic blast wave having traversed a gas cloud of density n_i=0.1 cm^{-3} and thickness 10^{16} cm. All other parameters are as in Fig.2. The Lorentz factor of the blast wave did virtually not change, hence repeated cloud crossings would produce the same spectra.

3 Radiation modelling of the blast wave

In the blast wave frame the external density $n_i = \Gamma\, n_i^*$ and sweep-up occurs at a rate

$$\dot{N}(\gamma) = \pi\, R^2\, c n_i^* \sqrt{\Gamma^2 - 1}\, \delta(\gamma - \Gamma)\ . \tag{9}$$

The sweep-up is a source of isotropic, quasi-monoenergetic protons and electrons with Lorentz factor Γ in the blast wave frame. The isotropisation also provides a momentum transfer from the ambient medium to the blast wave. In a time interval δt the blast wave sweeps up a momentum of $\delta\Pi = \pi\, R^2\, m_p\, c^2\, n_i^*\, (\Gamma^2 - 1)\, \delta t$ which is transferred from the swept-up particles to the whole system. Therefore, the blast wave Lorentz factor relative to the ambient medium reduces to

$$\Gamma' = \Gamma \sqrt{1 + \left(\frac{\delta\Pi}{M_{BW}\, c}\right)^2} - \sqrt{\Gamma^2 - 1}\, \frac{\delta\Pi}{M_{BW}\, c} \tag{10}$$

which can easily be integrated numerically. Equation (9) states the differential injection of relativistic particles in the blast wave. Here we concentrate on the protons because they receive a factor of m_p/m_e more power than electrons, which also have a low radiation efficiency for $\gamma \ll 1000$. Electrons (and positrons) are supplied much more efficiently as secondary particles following inelastic collisions of the relativistic protons. Since no reacceleration is assumed, the continuity equations for particle i reads

$$\frac{\partial N_i(\gamma)}{\partial t} + \frac{\partial}{\partial \gamma}\Big(\dot{\gamma}\, N_i(\gamma)\Big) + \frac{N_i(\gamma)}{T_{ann}} = \dot{N}_i(\gamma) \tag{11}$$

where for positrons catastrophic annihilation losses on a timescale T_{ann} are taken into account. The injection rate of secondary electron is related to the rate of inelastic collisions. In Fig.2 we show the spectral evolution of high energy emission from a collimated blast wave for a homogeneous external medium. Even for very moderate ambient gas densities the high energy emission will be very intense. To this we oppose in Fig.3 the case of the blast wave interacting with an isolated gas cloud.

4 Conclusions

We have shown that a relativistic blast wave can sweep-up ambient matter via a two-stream instability which provides relativistic particles in the blast wave without requiring any acceleration process. The high energy emission thereby produced has characteristics typical of BL Lacertae objects. In particular,

– The high energy spectra are very hard with photon indices < 2, in accord with the unspectacular appearance of TeV-bright sources at GeV energies (Buckley et al. 1996)

– As can be seen in Fig.3, observable increase and decrease of intensity at TeV energies can be produced on sub-hour timescales, in accord with the observed variability time scales of Mkn 421 (Gaidos et al. 1996)

– For multiple outbursts the intensity follows the variation of the ambient gas density with little spectral variation, similar to the observed behaviour of Mkn 501 (Aharonian et al. 1999)

– X-ray synchrotron emission up to ≈ 100 keV is produced in parallel to the γ-rays , but may be slightly delayed compared to the TeV emission, as was observed from Mkn 501 (Pian et al. 1998).

References

Aharonian, F.A., Akhperjanian, A.G., Barrio, J.A. et al., 1999, A&A 342, 69

Böttcher, M., Dermer, C.D., 1998, ApJ 499, L131

Buckley, J.H., Akerlof, C.W., Biller, S. et al., 1996, ApJ 472, L9

Gaidos, J.A., Akerlof, C.W., Biller, S. et al., 1996, Nature 383, 319

Pian, E., Vacanti, G., Tagliaferri, G. et al. 1998, ApJ 492, L17

Schlickeiser R., 1989, ApJ 336, 243

Vietri, M., 1997, PRL 78, 4328

Waxman, E., 1997, ApJ 491, L19